EUROFUSION WPHCD-PR(15) 12903

Z.C. Ioanndis et al.

Open-ended Coaxial Cavities with Corrugated Inner and Outer Walls

Preprint of Paper to be submitted for publication in International Journal of Infrared, Millimeter and Terahertz Waves

This work has been carried out within the framework of the EUROfusion Consortium and has received funding from the Euratom research and training programme 2014-2018 under grant agreement No 633053. The views and opinions expressed herein do not necessarily reflect those of the European Commission.

Noname manuscript No.
(will be inserted by the editor)

Open-ended Coaxial Cavities with Corrugated Inner and Outer Walls

Zisis C. Ioannidis · Konstantinos. A. Avramidis · Ioannis. G. Tigelis

Received: date / Accepted: date

Abstract In this work an open-ended coaxial cavity with a corrugated insert and a relatively small number of corrugations on the outer wall is studied. In particular, the Spatial Harmonics Method (SHM) is employed in order to derive the TE modes characteristic equation, which is then solved by truncation for the calculation of the corresponding eigenvalues. Special care is given in the expansion functions used in order to avoid numerical instabilities in the calculation of high-order spatial terms. Various cases of outer wall corrugations are studied numerically in order to identify the effect of the outer corrugations and understand the mode coupling mechanism.

Keywords Gyrotron · coaxial cavities · corrugated waveguides · Spatial Harmonics Method

This work was partially supported by the Association Euratom-Hellenic Republic under PPP&T framework, Task agreements WP12-DAS-HCD and WP13-DAS-03-HCD and partially has been carried out within the framework of the EUROfusion Consortium and has received funding from the Euratom research and training programme 2014-2018 under grant agreement No 633053. The views and opinions expressed herein do not necessarily reflect those of the European Commission.

Zisis C. Ioannidis
Department of Electronics, Computers, Telecommunications and Control, Faculty of Physics, National and Kapodistrian University of Athens, 15784 Athens, Greece
Tel.: +302107276992
E-mail: zioanni@phys.uoa.gr

Konstantinos A. Avramides
Institute for Pulsed Power and Microwave Technology, Karlsruhe Institute of Technology, D-76131 Karlsruhe, Germany
E-mail: konstantinos.avramidis@kit.edu

Ioannis G. Tigelis
Department of Electronics, Computers, Telecommunications and Control, Faculty of Physics, National and Kapodistrian University of Athens, 15784 Athens, Greece
Tel.: +302107276860
E-mail: itigelis@phys.uoa.gr

1 Introduction

Coaxial waveguides and open-ended cavities, with corrugations on the inner conductor and smooth outer wall, as well as with smooth inner conductor and corrugated outer wall have been proposed and used in multiple industrial and scientific applications. Depending on the positioning, the number and the size of the corrugations, such kind of coaxial structures have been used extensively in vacuum tubes for microwave and millimetre wave generation and amplification.

The multi-segment magnetron is one of the most representative examples of microwave sources with a coaxial corrugated resonant system [1]. In these sources the inner conductor of the resonator, which serves as the cathode, is usually smooth and a small number of oversized corrugations is introduced on the outer wall, which is the anode. Due to the small number and the large dimensions of the corrugations, the latter are also refereed to as side cavities, side resonators or vanes. Although various shapes of such side resonators have been proposed, the wedge-shaped resonators are the most commonly used in magnetrons [2].

Similar structures, with relatively small number of corrugations, have been also proposed as the interaction region for gyro-TWTs and various studies address the cases of smooth inner conductor with vane loaded outer wall as well as smooth outer wall and longitudinally corrugated inner conductor [3], [4]. Although such structures do not provide broadening of the amplifier bandwidth, they compensate the gain loss that occurs other bandwidth broadening techniques, such as the tapering of the cross section and of the external magnetic field [5].

Of course, the introduction of longitudinal wedge-shaped corrugations is not limited in gyro-amplifiers and applies for gyro-oscillators too. Gradually tapered open-ended resonators are nowadays widely used in the development of gyrotrons for high-frequency high-power microwave generation [6], [7]. In these oscillators, a relatively large number of corrugations is introduced on the inner conductor, whereas the outer wall of the resonator remains smooth [8]. Selecting the inner conductor's radius and the corrugations properties properly, the eigenvalue spectrum of the cavity is significantly rearranged and the quality factors of the competing modes can be selectively changed, providing in this way an additional means for mode selection [9].

An additional idea to increase even more the mode-selectivity could be the additional introduction of a small number of wedge-shaped corrugations on the outer wall. Such a structure would work as a mode converter and could couple close neighboring azimuthal modes of a gyrotron cavity with lower-order modes with relatively small diffractive quality factors [10]. This structure gained attention lately [11], [12], however, in those works the mode coupling of the azimuthal modes, which would be the key element for the enhancement of the selectivity properties of the cavity, is neglected. This is because they supposed a large number of corrugations for both the inner and the outer walls and thus the Surface Impedance Model (SIM) is used.

In this work, we use a full-wave method to address the problem. In particular, the Spatial Harmonics Method (SHM) is employed to calculate the eigenvalue spectrum of TE modes in a coaxial cavity with corrugations on both the inner and the outer wall. In Section II, the fields are expanded in terms of spatial eigenfunctions, and the application of the appropriate boundary conditions at the interfaces leads to a homogeneous system of infinite equations, which is solved by truncation. In Section III various issues regarding the numerical implementation of the method are discussed. Then, in Section IV we present numerical results that highlight the way introduction of outer corrugations affects the eigenvalue spectrum of a typical coaxial cavity with corrugated insert yet smooth outer wall. Finally, we summarize our conclusions in Section V.

2 Mathematical Formulation

Fig. 1 presents the transverse cross-section of a coaxial cavity with inner and the outer radius R_i and R_o, respectively. Fig. 2 presents the unfolded unit cell of the same geometry. On the surface of the outer wall there are M wedge-shaped corrugations with depth D and additionally N of them with depth d, on the inner wall. Assuming that the ratio N/M is an integer number, the period of the structure is $\varphi_P = 2\pi/M$, defined by the number of corrugations on the outer wall. When the number of the inner corrugations is much larger than the number of the outer corrugations, this assumption is not limiting because N can be always selected accordingly. This is justified by [13] where it was shown that minor changes on the number of inner corrugations have almost no effect on the eigenvalue spectrum of a cavity, provided that the number of the inner corrugations N is relatively large. The angular corrugation parameter, defined as the ratio of the non-metallic part of the corrugation to the angular width of the unit cell of the corrugation, is φ_D/φ_P for the outer wall and φ_L/φ_S for the inner wall. Although the corrugations of each surface are identical between each other, the outer corrugations are in general different from the inner corrugations. In particular, we are interested in cases where the outer wall has a small number of wide corrugations, whereas the inner wall has a large number of relatively shallow surface corrugations. This is actually the reason, why the Surface Impedance Method should not be applied to study such a structure, as it cannot model correctly the outer corrugations.

In order to employ the SHM formulation, the structure is divided into three regions. *Region I* represents the propagation volume between the surface corrugations, *Region II* represents each of the inner corrugation slots, whereas *Region III* represents each of the outer corrugation slots. Due to the angular periodicity, the Floquet's theorem is applicable in *Region I* and the longitudinal component of the electric field is described as an infinite series of Bloch components in the azimuthal direction:

$$H_z^{\mathrm{I}} = \sum_{n=-\infty}^{+\infty} \left[A_n F_{k_n}\left(\frac{\chi r}{R_o}\right) + B_n G_{k_n}\left(\frac{\chi r}{R_o}\right) \right] e^{jk_n\varphi} \tag{1}$$

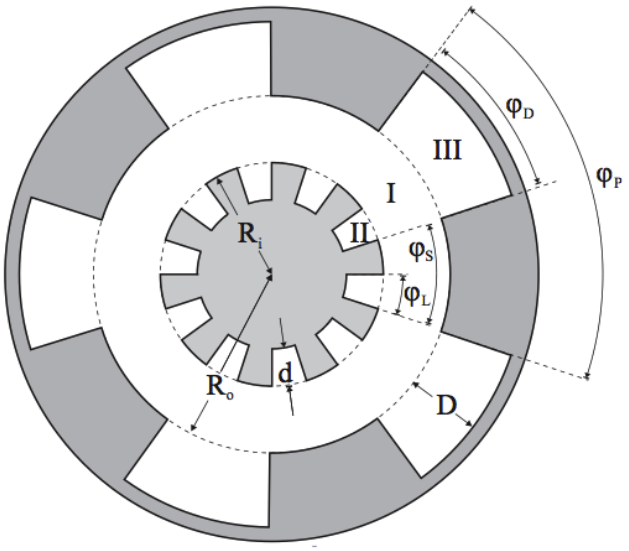

Fig. 1 Cross-section of a coaxial cavity with wedge-shaped corrugations on the surface of both the inner and the outer wall.

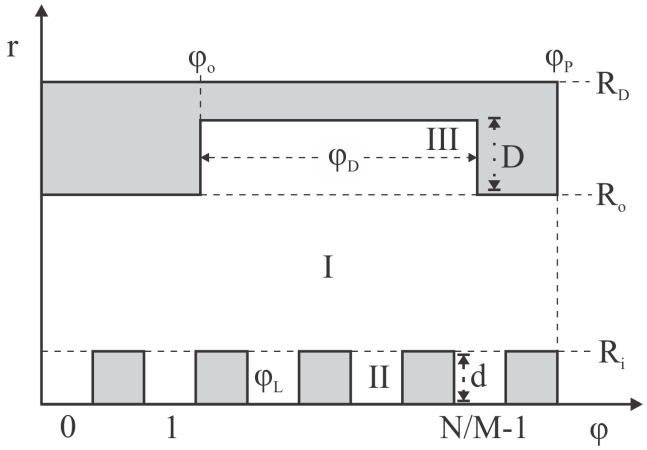

Fig. 2 Detail of unfolded unit cell of Fig. 1.

where $\chi = k_\perp R_o$ is the transverse wavenumber $k_\perp$ normalized to the outer radius R_o. Assuming that the fundamental azimuthal mode index is m, $k_n = m + nM$ is the wavenumber corresponding to the spatial harmonic n. A_n and B_n are unknown expansion coefficients to be found and the functions $F_n(a)$ and $G_n(a)$ are properly scaled Bessel functions of the first and second kind, respectively, given by:

$$F_n\left(a\right) = \mathrm{J}_n\left(a\right)/\mathrm{J}_n\left(\chi\right) \tag{2}$$

$$G_n(a) = \mathrm{Y}_n(a)/\mathrm{Y}_n\left(\frac{\chi}{C}\right) \tag{3}$$

where $C = R_o/R_i$ is the outer to inner radii ratio. It should be noted that the scaled functions (2) and (3) have been selected properly in order to avoid numerical issues even for very high orders.

In each slot of *Region II*, as well as in *Region III*, the longitudinal component of the magnetic field will be a summation of standing waves, i.e.:

$$H_z^{\mathrm{II}} = \sum_{\ell=0}^{+\infty} C_\ell^i Q_{k_\ell}\left(\frac{\chi r}{R_o}, \frac{\chi}{C_d}, \frac{\chi}{C}\right) \cos\left[k_\ell\left(\varphi - i\varphi_S\right)\right] \tag{4}$$

$$H_z^{\mathrm{III}} = \sum_{p=0}^{+\infty} D_p Q_{k_p}\left(\frac{\chi r}{R_o}, \frac{\chi}{C_D}, \chi\right) \cos\left[k_p\left(\varphi - i\varphi_o\right)\right] \tag{5}$$

where $k_\ell = \ell\pi/\varphi_L$ and $k_p = p\pi/\varphi_D$ are the transverse wavenumbers of *Region II* and *Region III*, respectively, C_ℓ^i with $i = 0, 1, ..., N/M - 1$ and D_p are unknown expansion coefficients, $C_d = R_o/R_d$, $C_D = R_o/R_D$, whereas the function $Q_\nu(a, b, c)$ is a properly scaled linear combination of Bessel functions of the first and second kind given by:

$$Q_\nu(a, b, c) = \frac{\mathrm{J}_\nu(a)\,\mathrm{Y'}_\nu(b) - \mathrm{J'}_\nu(b)\,\mathrm{Y}_\nu(a)}{\mathrm{J}_\nu(c)\,\mathrm{Y}_\nu(b) + \mathrm{J}_\nu(b)\,\mathrm{Y}_\nu(c)}. \tag{6}$$

Note that for all the longitudinal components of the magnetic field a $f(z)$ longitudinal field dependence has been assumed, as well as harmonic variation with time $\exp(j\omega t)$.

Substituting the longitudinal components in the Maxwell's equations we get the transverse components of the electromagnetic field in all regions. Then, applying the boundary conditions, which demand the continuity of the tangential components of the fields on the interface between the three regions ($r = R_o$ and $\varphi_o < \varphi < \varphi_o + \varphi_D$, $r = R_i$ and $i\varphi_S < \varphi < i\varphi_S + \varphi_L$), the homogeneous system of infinite equations is derived:

$$\sum_{q=-\infty}^{+\infty} A_q\left(Z_{nq}^{\mathrm{III}} - \delta_{nq} Z_n^{\mathrm{I}}\right) + B_q\left(Z_{nq}^{\mathrm{IV}} - \delta_{nq} Z_n^{\mathrm{II}}\right) = 0 \tag{7}$$

$$\sum_{q=-\infty}^{+\infty} A_q\left(N_{nq}^{\mathrm{III}} - \delta_{nq} N_n^{\mathrm{I}}\right) + B_q\left(N_{nq}^{\mathrm{IV}} - \delta_{nq} N_n^{\mathrm{II}}\right) = 0 \tag{8}$$

The infinite system of (7) and (8) (see Appendix A for notation) can be also presented in the simpler form:

$$\mathbf{X} \cdot \mathbf{D} = \mathbf{0}, \tag{9}$$

where $\mathbf{X}$ is a vector that represents the unknown expansion coefficients A_n and B_n, whereas $\mathbf{D}$ is a square matrix with infinite dimensions whose components are given from (13)-(29) summarized in Appendix A. The expansion

coefficients for field distributions in *Region II* and *Region III* are related to A_n and B_n as:

$$C_\ell^i = \frac{2\sum_{n=-\infty}^{+\infty}\left[A_n F_{k_n}\left(\frac{\chi}{C}\right) + B_n G_{k_n}\left(\frac{\chi}{C}\right)\right] I_5}{Q_{k_\ell}\left(\frac{\chi}{C}, \frac{\chi}{C_d}, \frac{\chi}{C}\right)\varphi_L\left(1+\delta_{\ell 0}\right)} \tag{10}$$

$$D_p = \frac{2\sum_{n=-\infty}^{+\infty}\left[A_n F_{k_n}\left(\chi\right) + B_n G_{k_n}\left(\chi\right)\right] I_6}{Q_{k_\ell}\left(\chi, \frac{\chi}{C_D}, \chi\right)\varphi_D\left(1+\delta_{p 0}\right)}. \tag{11}$$

Non-trivial solutions for the expansion coefficients in (9) demand the determinant of $\mathbf{D}$ to be equal to zero, i.e.

$$|\mathbf{D}(\chi)| = 0. \tag{12}$$

Setting in (12) a specific value for the azimuthal index m, the eigenvalues $\chi = \chi_{mt}$, $t = 1, 2, \ldots$, are calculated. Then, for any specific eigenvalue the system (9) is solved for the calculation of the unknown expansion coefficients A_n and B_n.

3 Numerical Implementation

In order to calculate the determinant in (12) numerically we have to truncate the infinite system of equations (7) and (8) to a maximum value, which in practice means that we have to take into account a finite number of expansion terms in expressions (1), (4) and (5). In particular, the total number of expansion terms used for *Region I* is limited to those with indexes from $-n_{max}$ to n_{max}, whereas the summations in each part of *Region II* and *Region III* are limited to terms with indexes up to ℓ_{max} and p_{max}, respectively.

Although, the integers n_{max}, ℓ_{max} and p_{max} are all independent variables of the problem, the applications of SHM in similar eigenvalue problems [14], [15] has led to the empirical rule $\ell_{max} = p_{max} = 2n_{max}$, i.e $2n_{max}+1$ terms are taken into account in each neighboring region. Regarding n_{max}, it is increased gradually and the eigenvalues of interest are calculated until the desirable accuracy between two subsequent calculations is achieved. It should be noted that usually more expansion terms are needed to achieve fields convergence than to achieve eigenvalue convergence.

Recall that it has been already shown in [13] for a coaxial cavity with inner corrugations that due to the presence of the surface corrugations the azimuthal modes of the corresponding smooth structure (neglecting the inner and outer corrugations) are coupled. Thus, in order to calculate the eigenvalue spectrum up to the eigenvalue $\chi_{mp}(C)$ we should take into account at least those expansion terms that satisfy the criterion $|m + n \cdot N| \leq \chi_{mp}$, where m is the azimuthal index of the mode of interest, $n = -n_{max} \ldots n_{max}$ and N is the number of the inner wall corrugations [13]. Following the same procedure with the one presented in Section IV in [13], it can be shown that in a cavity with corrugations on both walls and $M < N$, we have to take into account

at least those expansion coefficients that satisfy $|m + n \cdot M| \leq \chi_{mp}$, where M is the number of the outer wall corrugations. The aforementioned procedure is omitted here, since it can be derived from [13] in a straightforward way. However, all the calculations in Section 4 satisfy this criterion unless stated differently. Note that since the number of the inner corrugations N in an integer multiple of the number of the outer corrugations M and $M < N$ the criterion $|m + n \cdot M| \leq \chi_{mp}$ ensures that all the proper coupled terms will be taken into account for the outer corrugations too.

Summarizing, n_{max} is selected to be at least as large as the criterion $|m + n \cdot M| \leq \chi_{mp}$ indicates in order to account for the coupled modes and then it is increased properly to obtain the preferable accuracy in the calculation of the eigenvalue curve under interest.

4 Numerical Results

We use the semi-analytical model presented in the previous sections to study the rearrangement of the eigenvalue curves of TE modes in coaxial waveguides with corrugated inner and outer walls. The parameters that we selected are primary for illustrative reasons. However, they are quite representative of coaxial cavities that are frequently used in high-power high-frequency gyrotron oscillators. In this context, we consider a coaxial structure having $N = 88$ surface slots on the inner conductor with relative corrugation depth $d/R_o = 0.015$ and angular ratio $\varphi_L/\varphi_S = 0.5$. In this geometry we introduce various types of outer wall corrugations and we study the rearrangement of the eigenvalue spectrum of the TE mode with azimuthal index $m = 28$.

4.1 Effect of the outer to inner corrugation number ratio

As it was mentioned in Section 2, our formulation is suitable for integer N/M ratios. For this reason we consider two different cases, where we introduce $M = 22$ and $M = 44$ corrugations on the outer wall of the above described structure, both with relative depth $D/R_o = 0.01$. In both cases we calculate the eigenvalue curves of TE modes with azimuthal index $m = 28$ with respect to the outer to inner radius ratio $C = R_o/Ri$. Note that we prefer to present the eigenvalues with respect to the C-ratio in order our results to be directly comparable with the eigenvalues of a coaxial structure without corrugations.

Fig. 3 presents the eigenvalue curves of TE modes with $m = 28$ (black squares) for the case of $M = 44$ outer slots. It is easy to recognize in this figure that there are two sets of similar curves. Moreover it is evident that both sets of curves have regions where their slope is positive and they form the, so called, inner mode [8]. Having these in mind, we could say that the eigenvalue spectrum of the complex structure with the inner and outer corrugations consists of a combination of the TE modes in the corresponding coaxial structure with inner corrugations only. The specific modes that are combined can be

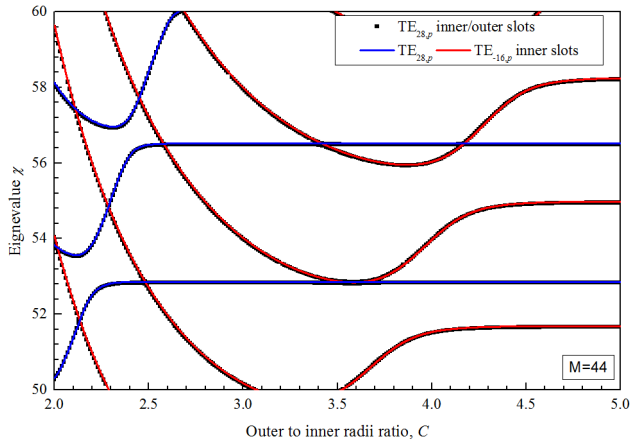

Fig. 3 Eigenvalue curves of TE modes with azimuthal index $m = 28$ (black squares) in a coaxial cavity with $N = 88$ and $M = 44$ corrugations on the inner and the outer wall, respectively, $d/R_o = 0.015$, $D/R_o = 0.01$, $\varphi_L/\varphi_S = \varphi_D/\varphi_P = 0.5$. The solid colored lines correspond to the eigenvalue curves in a coaxial corrugated structure with smooth outer wall for the cases of $m = 28$ (blue lines) and $m = -16$ (red lines).

identified from the transverse wavenumber $k_n = m + nM$. Indeed, piloting in the same figure with coloured solid lines the eigenvalue curves of the modes with azimuthal index $m = 28$ (blue lines) and $m = -16$ (red lines), in a coaxial corrugated structure with smooth outer wall, we get a perfect match.

Of course, as it was described in detail in [13], the eigenvalue spectrum of TE modes in a coaxial structure with inner corrugations consists of a combination of the modes in the corresponding smooth coaxial structure (no corrugations). The coupled modes can be easily identified by the different values of the transverse wavenumber $k_n = m + nN$. Thus, from another point of view, one could say that both the inner and the outer corrugations evoke azimuthal coupling of the modes of the smooth coaxial structure and the eigenvalue spectrum of the complex cavity is the combination of all the modes that are coupled due to both surface corrugations. Although the latter approach seems simpler, we prefer to address the coupling scheme progressively and in particular to think the spectrum of the complex structure as a combination of modes in the structure with the coaxial corrugated insert. This scheme is even more appropriate for cases with large number of inner corrugations N, where the coupled modes are located relatively high in the spectrum and far away from the χ-range of interest.

Fig. 4 presents the eigenvalues curves of TE modes with $m = 28$ in a coaxial structure with $M = 22$ outer and $N = 88$ inner corrugations. In the same figure we have plotted with colored lines the TE modes of the corresponding structure with a corrugated insert and smooth outer wall. It is evident that in this case the spectrum is more dense and this is due to the smaller number of outer corrugation that couples modes that are closer in azimuthal index.

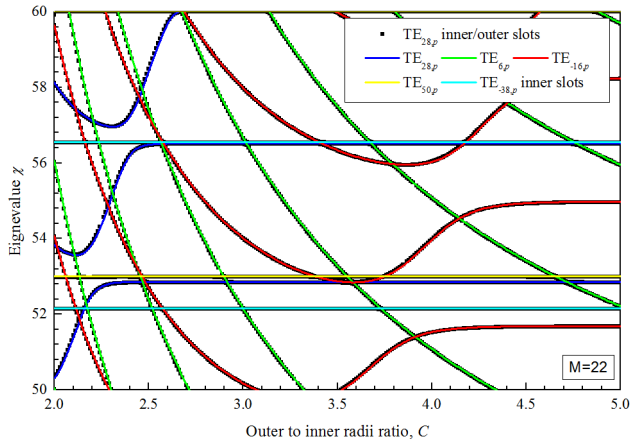

Fig. 4 Eigenvalue curves of TE modes with azimuthal index $m = 28$ (black squares) in a coaxial cavity with $N = 88$ and $M = 22$ corrugations on the inner and the outer wall, respectively, $d/R_o = 0.015$, $D/R_o = 0.001$, $\varphi_L/\varphi_S = \varphi_D/\varphi_P = 0.5$. The solid colored lines correspond to the eigenvalue curves in a coaxial corrugated structure with smooth outer wall for the cases of $m = 28$ (blue), $m = 6$ (green) $m = -16$ (red), $m = 50$ (yellow) and $m = -38$ (cyan).

For clarity reasons it is worthwhile to mention again that when we refer to the mode $\mathrm{TE}_{m,p}$ of a coaxial cavity with inner corrugations and smooth outer wall, we refer to the mode whose fundamental spatial term corresponds to azimuthal index m.

It should be noted here that if we followed a simplified method, such as SIM, we would not be able to account for the higher-order coupled terms and the representation of the eigenvalue spectrum would be questionable, since SIM assumes an infinite number of corrugations N and M.

Summarizing, it is clear that the number of the outer corrugations defines the modes that will be azimuthally coupled and may be used to bring in the eigenvalue range of interest additional modes. These modes can be easily identified from the different values that the transverse wavenumber k_n attains.

4.2 Effect of the outer corrugation depth

In the first part of Section 4 we kept the outer corrugations depth relatively low in order to avoid changing the eigenvalue curves significantly and focus on the effect of their number M. Fig. 5 presents the eigenvalue curves of TE modes with $m = 28$, in a coaxial structure with $N = 88$ inner and $M = 44$ outer corrugations, $\varphi_L/\varphi_S = \varphi_D/\varphi_P = 0.5$, $d/R_i = 0.015$ and having the relative corrugation depth D/R_o as parameter, with values $0.001 \leq D/R_o \leq 0.01$.

It is evident that increasing the corrugation depth the coupled modes move away from each other. Consequently, the distance between two coupled modes can be used to gain insight about the intensity of the coupling that the outer

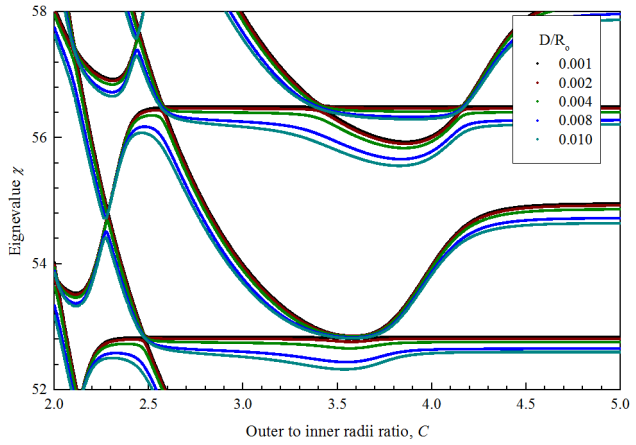

Fig. 5 Eigenvalue curves of TE modes with azimuthal index $m = 28$ (black squares) in a coaxial cavity with $N = 88$ and $M = 44$ corrugations on the inner and the outer wall, respectively, $\varphi_L/\varphi_S = \varphi_D/\varphi_P = 0.5$, $d/R_i = 0.015$ and the relative outer corrugation depth D/R_o as parameter.

corrugations evoke. Thus, when the introduction of the corrugations aims to couple specific modes without changing their eigenvalue curves significantly, the relative outer corrugation depth has to be kept relatively low

4.3 Effect of the outer corrugation angular ratio

Fig. 6 presents the eigenvalue curves with $m = 28$ in the same structure with $D/R_o = 0.12$ and the relative angular width φ_D/φ_P as parameter in the range $0.1 \leq \varphi_D/\varphi_P \leq 0.9$. In order to present clearly the effect of the later parameter we focused in the area where $3.0 \leq C \leq 4.0$ and $52.6 \leq \chi \leq 53.0$.

It can be seen in this figure that increasing the φ_D/φ_P-value progressively from 0.1 to 0.9 the eigenvalue curves move to lower χ-values. This shall be attributed to the fact that for the limiting cases of $\varphi_D/\varphi_P \approx 0$ and $\varphi_D/\varphi_P \approx 1$ we have in practice a smooth outer wall with radii R_o and R_D, respectively. Since $R_D \geq R_o$, the resonating volume of the structure increases and this is why the eigenvalue, i.e the eigenfrequency, drops. Moreover, it is easy to observe that from $\varphi_D/\varphi_P = 0.1$ and moving towards $\varphi_D/\varphi_P \approx 0.5$ the distance between the neighboring modes increases, revealing a similar increase in their coupling intensity. Then, moving from $\varphi_D/\varphi_P \approx 0.5$ to $\varphi_D/\varphi_P = 0.9$ the eigenvalue curves approach each other again and the coupling intensity is expected to decrease.

Although for manufacturing simplicity we would expect to use outer corrugations with $\varphi_D/\varphi_P = 0.5$, Fig. 6 shows that the relative angular ratio provides an additional means for the manipulation of the eigenvalue curves.

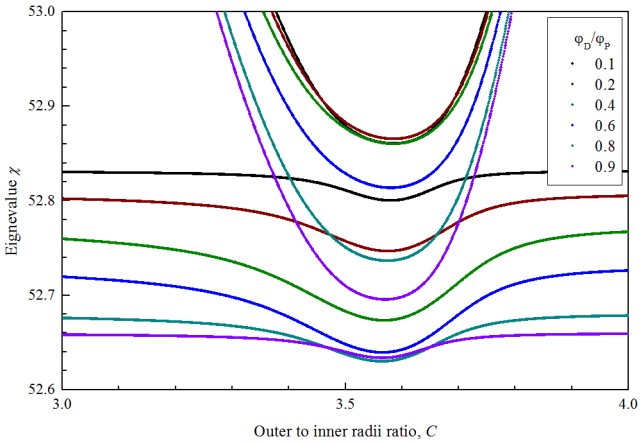

Fig. 6 Eigenvalue curves of TE modes with azimuthal index $m = 28$ in a coaxial cavity with $N = 88$ and $M = 44$ corrugations on the inner and the outer wall, respectively, $\varphi_L/\varphi_S = 0.5$, $d/R_i = 0.015$, $D/R_o = 0.12$ and the relative outer corrugation depth φ_D/φ_P as parameter.

5 Conclusion

We presented a full-wave approach to calculate the eigenvalues in a coaxial structure having corrugations both on the inner and the outer wall. Is was shown by example that the outer corrugations complicate the spectrum by coupling the modes of the coaxial structure with a corrugated insert and smooth outer wall. The modes that get coupled depend on the number of the corrugations and can be foreseen from the different values of the transverse wavenumber. Moreover, the outer corrugation depth d/R_o and the angular ratio φ_D/φ_P can be used to control the shape of the eigenvalue curve of interest.

It is worthwhile to mention again that the mode coupling phenomena that exist in such a complex structure can be only address with full-wave approaches. Thus, the validity of SIM based results is questionable and should be examined carefully.

A Formulation Notation Appendix

Herein we present the expressions of all quantities used in the mathematical formulation of Section 2. In particular:

$$Z_n^{\mathrm{I}} = \varphi_P \mathrm{F}'_{k_n}(\chi) \tag{13}$$

$$Z_n^{\mathrm{II}} = \varphi_P \mathrm{G}'_{k_n}(\chi) \tag{14}$$

$$Z_{nq}^{\mathrm{III}} = \frac{2\mathrm{F}_{k_q}(\chi)\, S_{nq}^{\mathrm{I}}}{\varphi_D} \tag{15}$$

$$Z_{nq}^{\mathrm{IV}} = \frac{2\mathrm{G}_{k_q}(\chi)\, S_{nq}^{\mathrm{I}}}{\varphi_D} \tag{16}$$

$$S_{nq}^{\mathrm{I}} = \sum_{p=0}^{+\infty} \frac{Q'_{k_p}\left(\chi, \frac{\chi}{C_D}, \chi\right)}{Q_{k_p}\left(\chi, \frac{\chi}{C_D}, \chi\right)} \frac{I_1 I_2}{1+\delta_{p0}} \tag{17}$$

$$N_n^{\mathrm{I}} = \varphi_P \mathrm{F}'_{k_n}\left(\frac{\chi}{C}\right) \tag{18}$$

$$N_n^{\mathrm{II}} = \varphi_P \mathrm{G}'_{k_n}\left(\frac{\chi}{C}\right) \tag{19}$$

$$N_{nq}^{\mathrm{III}} = \frac{2\mathrm{F}_{k_q}\left(\frac{\chi}{C}\right) S_{nq}^{\mathrm{II}}}{\varphi_L} \tag{20}$$

$$N_{nq}^{\mathrm{IV}} = \frac{2\mathrm{G}_{k_q}\left(\frac{\chi}{C}\right) S_{nq}^{\mathrm{II}}}{\varphi_L} \tag{21}$$

$$S_{nq}^{\mathrm{II}} = \sum_{i=0}^{\frac{N}{M}-1} \sum_{\ell=0}^{+\infty} \frac{Q'_{k_\ell}\left(\frac{\chi}{C}, \frac{\chi}{C_d}, \frac{\chi}{C}\right)}{Q_{k_\ell}\left(\frac{\chi}{C}, \frac{\chi}{C_d}, \frac{\chi}{C}\right)} \frac{I_3 I_4}{1+\delta_{\ell 0}} \tag{22}$$

$$I_1 = I\left(k_q, k_p, \varphi_o, \varphi_o + \varphi_D\right) \tag{23}$$

$$I_2 = I\left(-k_n, k_p, \varphi_o, \varphi_o + \varphi_D\right) \tag{24}$$

$$I_3 = I\left(k_q, k_\ell, i\varphi_S, i\varphi_S + \varphi_L\right) \tag{25}$$

$$I_4 = I\left(-k_n, k_\ell, \varphi_S, i\varphi_S + \varphi_L\right) \tag{26}$$

$$I_5 = I\left(k_n, k_\ell, i\varphi_S, i\varphi_S + \varphi_L\right) \tag{27}$$

$$I_6 = I\left(k_n, k_p, \varphi_o, \varphi_o + \varphi_D\right) \tag{28}$$

$$I\left(a, b, \varphi_1, \varphi_2\right) = \int_{\varphi_1}^{\varphi_2} e^{ja\varphi} \cos\left[b\left(\varphi - \varphi_1\right)\right] d\varphi \tag{29}$$

References

1. A. W. Hull: The effect of a uniform magnetic field on the motion of electrons between coaxial cylinders. Phys. Rev. **18**, 31–57 (1921)
2. N. Kroll: The unstrapped resonant system. In: G.B. Collins (ed.) Microwave Magnetrons, pp. 49–82. McGraw-Hill, New York (1948)
3. K. Singh, P. K. Jain, N. Basu: Analysis of a coaxial waveguide corrugated with wedge-shaped radial vanes considering azimuthal harmonic effects. PIER **47**, 297–312 (2004)
4. G. Singh, S. Chandra, P. Bhaskar, P. Jain, B. Basu: Analysis of a vane-loaded gyro-TWT for the gain-frequency response. IEEE Trans. Plasma Sci. **32**(5), 2130–2138 (2004)
5. K. R. Chu, Y. Lau, L. Barnett, V. Granatstein: Theory of a wide-band distributed gyrotron traveling-wave amplifier. IEEE Trans. Electron Devices **28**(7), 866–871 (1981)
6. J.-P. Hogge, T. P. Goodman, S. Alberti, F. Albajar, K. A. Avramides, P. Benin, S. Bethuys, W. Bin, T. Bonicelli, A. Bruschi, S. Cirant, E. Droz, O. Dumbrajs, D. Fasel, F. Gandini, G. Gantenbein, S. Illy, S. Jawla, J. Jin, S. Kern, P. Lavanchy, C. Liévin, B. Marlétaz, P. Marmillod, A. Perez, B. Piosczyk, I. Pagonakis, L. Porte, T. Rzesnicki, U. Siravo, M. Thumm, M. Q. Tran: First experimental results from the European Union 2-MW coaxial cavity iter gyrotron prototype. Fusion Sci. and Technol. **55**(2), 204–212 (2009)
7. T. Rzesnicki, G. Gantenbein, J. Jelonnek, J. Jin, I. Pagonakis, B. Piosczyk, A. Samartsev, A. Schlaich, M. Thumm: 2 MW, 170 GHz coaxial-cavity short-pulse gyrotron - single stage depressed collector operation. In: Infrared, Millimeter, and Terahertz waves (IRMMW-THz), 2014 39th International Conference on, pp. 1–2 (2014)
8. C. T. Iatrou, S. Kern, A. B. Pavelyev: Coaxial cavities with corrugated inner conductor for gyrotrons. IEEE Trans. Microw. Theory Techn. **44**(1), 56–64 (1996)
9. C. T. Iatrou: Mode selective properties of coaxial gyrotron resonators. IEEE Trans. Plasma Sci. **24**(3), 596–605 (1996)

10. S. Kern, C. T. Iatrou, M. K. A. Thumm: Investigations on mode stability in coaxial gyrotrons. 17th International Conference on Infrared Millimeter and Terahertz Waves (IRMMW-THz) pp. 1–39 (1995)
11. A. Shenyong Hou, B. Sheng Yu, C. Hongfu Li, D. Qixiang Zhao, E. Xiang Li: Ohmic losses in coaxial resonators with longitudinal inner-outer corrugation. Physics of Plasmas (1994-present) **20**(5), 052104 (2013)
12. S. Hou, S. Yu, H. Li, Q. Zhao: Research on eigenvalue and ohmic loss of coaxial resonator with inner-outer corrugation. IEEE Trans. Plasma Sci. **42**(1), 73–78 (2014)
13. Z. C. Ioannidis, K. A. Avramides, G. P. Latsas, I. G. Tigelis: Azimuthal mode coupling in coaxial waveguides and cavities with longitudinally corrugated insert. IEEE Trans. Plasma Sci. **39**(99), 1213–1221 (2011)
14. G. P. Latsas, Z. C. Ioannidis, I. G. Tigelis: Dependence of parasitic modes on geometry and attenuation in gyrotron beam tunnels. IEEE Trans. Plasma Sci. **40**(6), 1538–1544 (2012)
15. Z. C. Ioannidis, O. Dumbrajs, I. G. Tigelis: Eigenvalues and ohmic losses in coaxial gyrotron cavity. IEEE Trans. Plasma Sci. **34**(4), 1516–1522 (2006)